

## CHEMISTRY

Vapour Pressures of Xenon (77°–180° K)  
and Krypton (77°–130° K)

For the evaluation of recently measured low-temperature adsorption data we required the vapour pressure curves of krypton and xenon from 77° K to about 20° K above their respective triple points. We therefore undertook a critical review of the literature in order to try to define for each gas the vapour pressure curve that is best substantiated by the reported values. We found that the vapour pressure data for krypton published by various authors<sup>1-6</sup> are generally in good agreement with each other. Most reported values lie within  $\pm 1$  per cent of the curve given by the vapour pressure equations of Freeman and Halsey<sup>6</sup>, which can therefore be used with some confidence.

On the other hand, the vapour pressure data for xenon<sup>3,6-9</sup> show more serious inconsistencies, and the use of the equations recommended for solid xenon in different temperature regions results in a sharp change in the slope of the curve of  $\ln p$  against  $1/T$  when changing over from one equation to the next, although it is clear that no corresponding phase change of the condensed xenon occurs.

We have therefore examined the available vapour pressure data for xenon and compared them with the vapour pressure curve, which can be calculated from calorimetric data<sup>10</sup>, in an attempt to find a satisfactory smooth curve from 77° K to 180° K. The vapour pressure equations considered are given in Table 1.

The *FH* equation for liquid xenon deviates quite considerably, especially towards 180° K, from those of *HO* and *MW*, which agree with each other within 0.5 per cent. For solid xenon, the temperature regions of the two available vapour pressure equations (*FH* and *PD*) do not overlap; extrapolation of the *PD* equation yields an intersection point at 111.5° K, where, however, solid xenon exhibits no phase change.

A first indication of the reliability of the slopes of the vapour pressure equations near the triple point is obtained from Table 2 in which the Clapeyron melting enthalpies calculated from the difference in slopes of the vapour pressure equations at the triple point are compared to the calorimetrically measured values<sup>10,11</sup>. It is inferred that it is probable that the slopes of *HO* (and therefore of *MW*) and of *FH* for the solid are close to the true ones, whereas the slope of the *FH* liquid equation is erroneous. For krypton the two *FH* equations yield a value which is in reasonable agreement with the calorimetric one.

Table 1. VAPOUR PRESSURE EQUATIONS FOR XENON

Vapour pressure equation ( <i>p</i> ) (mm Hg)	Stated temperature range in which equation valid (°K)	Authors and abbreviations used in text
$\text{Log}_{10} p = 7.2488 - \frac{720.7}{T}$	160.56–166.2	Freeman and Halsey* ( <i>FH</i> )
$\text{Log}_{10} p = 6.9903 - \frac{678.49}{T}$	160.8–166.0	Heuse and Otto* ( <i>HO</i> )
$\text{Log}_{10} p = 26.08413 - \frac{1.040.76}{T} - 8.25369 \log_{10} T + 0.0085216 T$	161.7–289.2	Michels and Wassenaar* ( <i>MW</i> )
$\text{Log}_{10} p = 7.7371 - \frac{799.1}{T}$	110.0–160.56	Freeman and Halsey* ( <i>FH</i> )
$\text{Log}_{10} p = 8.044 - \frac{833.33}{T}$	70 – 90	Podgurski and Davis* ( <i>PD</i> )

\* Equation obtained from their data with the method of least squares.

Table 2. COMPARISON OF CALORIMETRIC AND CLAPEYRON MELTING ENTHALPIES

	Calorimetric (cal/mole)	Clapeyron from <i>FH</i> equations (cal/mole)	Clapeyron from <i>FH</i> and <i>HO</i> equations (cal/mole)
Kr	390.7 (ref. 11)	401	—
Xe	548.5 (ref. 10)	359	552

The calorimetric data of Clusius and Riccoboni<sup>10</sup> are extensive, and have been used to calculate a calorimetric vapour pressure curve with the equation:

$$\log_{10} p = 4.464 + 2.50 \log_{10} T - \frac{L_0}{4.576T} - \frac{\int_0^T \frac{c_p}{T} dT}{4.576} + \frac{\int_0^T c_p dT}{4.576T} - \frac{Bp}{4.576T}$$

The last term is only significant above 120° K. It is a correction term for the non-ideal behaviour of the saturated vapour which is assumed to obey the equation of state,  $pV = RT + Bp$ , where:

$$B = \frac{9}{128} \frac{RT_c}{p_c} \left( 1 - 6 \frac{T_c^2}{T^2} \right)$$

from the Berthelot equation. In Fig. 1 it is shown how, using a value for the latent heat of sublimation of xenon at 0° K ( $L_0$ ) of 3,780 cal/mole, which is also the value recommended by Hollis Hallett<sup>12</sup>, the calorimetric vapour

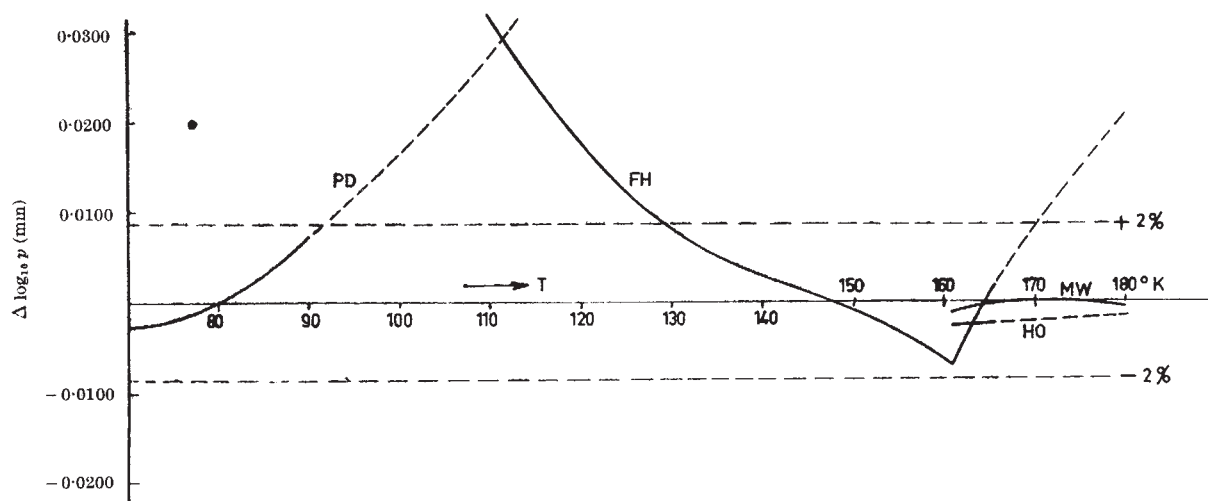


Fig. 1. Deviation of experimental xenon vapour pressure equations from calorimetric vapour pressure curve. ●, Liang (ref. 3); --- equation extrapolated outside experimental temperature region or stated region of validity

pressure curve deviates from the vapour pressure data available between 77° and 180° K.

It can be seen that for liquid xenon the *MW* and *HO* vapour pressure equations agree well with the calorimetric curve. For solid xenon the *PD* equation is in agreement within its stated experimental accuracy in the experimental temperature region but when extrapolated to higher temperatures it begins to deviate seriously. The *FH* equation agrees (within 2 per cent) with the calorimetric equation only at temperatures above 130° K. The value given by Liang<sup>3</sup> falls off by 5 per cent. It is possible that this deviation is due to uncertainty in the thermal transpiration correction as has been discussed by Podgurski and Davis<sup>9</sup>.

We therefore recommend that, until more precise vapour pressure measurements are available, the calorimetric vapour pressure curve should be used for the vapour pressure of solid xenon. The estimated error is  $\pm 2$  per cent at any temperature between 70° and 161° K. The vapour pressure is most easily calculated from the values given by the *PD* or *FH* equation and by the application of the correction curve given by Table 3. For the vapour pressure of liquid xenon either the *MW* or, below 180° K, the *HO* equation can be used.

Table 3. CORRECTIONS TO BE APPLIED TO THE *PD* OR *FH* EQUATIONS TO OBTAIN THE VAPOUR PRESSURE OF SOLID XENON

<i>T</i> (°K)	<i>p</i> (mm Hg)	Log <sub>10</sub> ( <i>p</i> )
70	$1.39 \times 10^{-4}$	<i>PD</i> + 0.0028
80	$4.24 \times 10^{-4}$	<i>PD</i> + 0.0000
90	$5.99 \times 10^{-4}$	<i>PD</i> - 0.0072
100	$4.95 \times 10^{-4}$	<i>PD</i> - 0.0164
110	2.76	<i>PD</i> - 0.0275
		<i>FH</i> - 0.0320
120	11.5	<i>FH</i> - 0.0173
130	33.2	<i>FH</i> - 0.0085
140	106	<i>FH</i> - 0.0030
150	258	<i>FH</i> + 0.0010
160	562	<i>FH</i> + 0.0067

We thank the O.E.C.D. High Temperature Reactor Project *Dragon*, the sponsors of our low-temperature adsorption investigations, for permission to publish this communication.

A. GRÜTTER  
J. C. SHORROCK

Battelle Memorial Institute,  
Geneva.

<sup>1</sup> Meihuizen, J. J., and Crommelin, C. A., *Physica*, **4**, 1 (1937).

<sup>2</sup> Michels, A., Wassenaar, T., and Zwietering, T. N., *Physica*, **18**, 63 (1952).

<sup>3</sup> Liang, S. Chu, *J. App. Phys.*, **22**, 148 (1951).

<sup>4</sup> Fisher, B. B., and MacMillan, W. G., *J. Phys. Chem.*, **62**, 494 (1958).

<sup>5</sup> Keesom, W. A., Mazur, J., and Meihuizen, J. J., *Physica*, **2**, 669 (1935).

<sup>6</sup> Freeman, M. P., and Halsey, G. D., *J. Phys. Chem.*, **60**, 1119 (1956).

<sup>7</sup> Heuse, W., and Otto, J., *Z. Tech. Physik*, **13**, 277 (1932).

<sup>8</sup> Michels, A., and Wassenaar, T., *Physica*, **16**, 253 (1950).

<sup>9</sup> Podgurski, H. H., and Davis, F. N., *J. Phys. Chem.*, **65**, 1343 (1961).

<sup>10</sup> Clusius, K., and Riccoboni, L., *Z. Phys. Chem. (Leipzig)*, **B38**, 81 (1938).

<sup>11</sup> Clusius, K., *Z. Phys. Chem. (Leipzig)*, **B31**, 459 (1936).

<sup>12</sup> Hollis Hallett, A. C., in *Argon, Helium and the Rare Gases*, edit. by Cook, G. A., **1**, 350 (Interscience, New York, 1961).

## Water Content of Black Soap Films

In a recent investigation of the thickness of black soap films, Corkill *et al.*<sup>1</sup> determined the water content of the films by measuring the absorption of radiation at 2.93 $\mu$  by placing a number of black films in an infra-red beam. In order to calculate the amount of water from the infra-red absorption, it is necessary to know the molar extinction coefficient at 2.93 $\mu$ . Since the absorption is so strong, Corkill *et al.* measured the extinction coefficient with very thin cells (using a gold leaf spacer) and claim that the value of 133 obtained by this method was identical with the extinction coefficient obtained by measuring the optical density of water in deuterium oxide. There is no reason to suppose that the extinction coefficient should be

identical for pure water and dilute water in deuterium oxide, and a re-determination was considered desirable, particularly as the value of 133 quoted by Corkill *et al.* is very different from the earlier value of 55 obtained by Fox and Martin<sup>2</sup>.

The full experimental details for the determination of the molar extinction coefficients will be given elsewhere<sup>3</sup>; but it is found that the value for water in D<sub>2</sub>O is 131, in good agreement with Corkill *et al.*, but that the value for pure water in thin films is 81. This difference between pure water and water in D<sub>2</sub>O is reasonable and will be discussed later<sup>3</sup>. Taking the value of 81, the amount of water in the black soap films examined by Corkill *et al.* will be larger by a factor of 1.62 than the values quoted by these authors. Thus for a film drawn from an aqueous solution of C<sub>10</sub>H<sub>21</sub>N(CH<sub>3</sub>)<sub>3</sub>C<sub>10</sub>H<sub>21</sub>SO<sub>4</sub> ( $8 \times 10^{-4}$  M) + NaBr (0.5 M) said to be 72 Å thick with a water core of 29.4 Å, the corrected water core thickness would be 47.6 Å. However, this calculation is open to objections. The extinction coefficient is certainly a function of the composition of the water phase, in the same way as the Raman intensities for the water vibration band are a function of the solute concentration and type in aqueous solutions<sup>4,5</sup>.

We thank Dr. W. A. Senior for his advice.

W. K. THOMPSON  
B. A. PETHICA

Chemical Physics Division,  
Unilever Research Laboratory,  
Port Sunlight.

<sup>1</sup> Corkill, J. M., Goodman, J. F., Ogden, C. P., and Tate, J. R., *Proc. Roy. Soc. A*, **273**, 84 (1963).

<sup>2</sup> Fox, J. J., and Martin, A. E., *Proc. Roy. Soc. A*, **174**, 235 (1940).

<sup>3</sup> Thompson, W. K. (to be published).

<sup>4</sup> Schultz, J. W., and Hornig, D. F., *J. Phys. Chem.*, **65**, 2131 (1961).

<sup>5</sup> Clifford, J., Senior, W. A., and Pethica, B. A., *Conf. Forms of Water in Biologic Systems* (N.Y. Acad. Sci., New York, October 1964).

## Nucleation and Morphology of Chymotrypsinogen Crystals

It has been suggested recently<sup>1</sup> that the morphology of enzyme crystals grown from solutions at various supersaturations<sup>2</sup> may be interpreted in terms of the basic mechanisms of nucleation. Little is known of either the nucleation mechanism or the solid-state properties of enzymes, since most are notoriously unstable even under mild conditions. The work presented here is a preliminary examination of the nucleation of bovine  $\alpha$ -chymotrypsinogen from solution. This enzyme has been selected because it is available commercially in a particularly pure form and something is known of its solid-state structure. From X-ray diffraction data<sup>3</sup> the molecule is said to be spherical with a radius of 21 Å. It consists of approximately 246 amino-acid units<sup>4</sup> and has a molecular volume of 17,100 ml./mole<sup>5</sup>.

If an aqueous solution of chymotrypsinogen is allowed to evaporate on a glass slide at a temperature of about 20° C very small crystallites are produced. Using carbon films and platinum shadowing it is possible to examine the morphology of replicas by low-magnification electron microscopy, some typical examples being shown in Figs. 1, 2 and 3. The crystals are generally in the size-range 1–10 $\mu$  and the morphology shows several apparently familiar features with some unusual details. Fig. 1 indicates a collapsed pyramid structure similar to that known for several synthetic polymers in which chain folding is the dominant growth mechanism, and Fig. 3 shows dendritic growth with a marked central groove. Despite a search of many such crystals with high-resolution electron microscopy we have been unable to detect screw dislocations or regular growth steps. Although the absence of these features seems to indicate that chain folding is not the normal growth mechanism it could also